TECHNISCHE MECHANIK, Band 23, Heft 2-4, (2003), 167– 177
Manuskripteingang: 13. Juni 2003

Homogenisation of Microheterogeneous Materials Considering Interfacial Delamination at Finite Strains *

S. Löhnert, P. Wriggers

In modern engineering, composite materials gained importance because of their specific properties requested by the individual application. They consist of inclusions such as particles or fibres which are introduced into a binding matrix material in order to "design" special material behaviour. In case of particle inclusions, typical materials are concrete, aluminum-boron or rubber filled with carbon. Fibre reinforced composites are typically stiffened by glass-, carbon- or aramid fibres. Recently, fibre reinforced metals are also subject to detailed investigation and application. In all cases the mechanical behaviour on the micro level defines the resulting material behaviour on the macro scale, which is needed from an engineering point of view in an arbitrary design process. The effective properties of the overall material depend on the geometry of the microstructure and the material properties of the constituents. In case of finite strains one can observe interfacial degradation in a cohesive zone between the matrix material and the inclusions. In this paper we focus on the homogenisation process of such materials with interfacial delamination. Here the difficulties arise from the geometrical and material nonlinearities. Even for linear elasticity this homogenisation can hardly be done analytically. Therefore we apply the finite element method to get a numerical approximation for the mechanical behaviour of a representative volume element (RVE). The homogenisation then is done with a statistically representative set of RVEs. In order to increase the efficiency and accuracy of the computations the finite element meshes are refined adaptively using non-conforming elements.

1 Introduction

Modern engineering applications have been substantially improved by the use of composite materials designed to provide the desired mechanical behaviour. Such composite materials consist of a binding matrix and inclusions such as particles or fibres. Most often the purpose of those inclusions is to stiffen the material. Unfortunately for normal engineering applications one doesn't know the detailed microstructure of the material, and even if, it would hardly be possible to compute the whole component using all the details. Thus it is necessary to homogenise the microstructure, get all the necessary information for the effective material behaviour of the homogenised material and use this data to compute the macroscopic component. This homogenisation process is done on a representative volume element (RVE) which - as the name already says - is able to statistically represent the microstructure. For linear elastic materials first estimates for the behaviour of the homogenised material date back to the works of Voigt (1889) and Reuss (1929), and to the works of Hill (1952), Bishop and Hill (1951b) and Bishop and Hill (1951a) as well as to Eshelby (1957). Even for linear elastic material behaviour the effective material response to an applied load on a RVE can only be calculated analytically in very few special cases. In the 60s and 70s there were developed more precise bounds by Hashin and Shtrikman (1962) and also more precise estimates like the one from Mori and Tanaka (1973). Unfortunately it is not possible to compute the effective material response of a RVE with an arbitrary microstructure analytically. Thus recently numerical methods have been employed to get more precise results. For linear elastic materials including damage this has been done for example by Zohdi and Wriggers (2001). In general, due to bigger differences in the material data of the components of the microstructure locally there occur quite large deformations in the transition zone between the inclusion and the matrix material. This is also the case even when applying only small deformations on the boundary of the RVE. In this cohesive zone debonding and delamination phenomena due to large stresses can occur. In this paper we present a numerical method to efficiently compute the mechanical behaviour of a RVE under finite deformations including damage in the cohesive zone around the inclusions, and we homogenise the material behaviour of this RVE.

*Dedicated to the memory of J. Olschewski, for his cheerfulness and cooperation as a colleague and friend over many years

The effective material data of the RVE is obtained from the relation between the effective stresses and the effective strains. This means that the effective material tensor $\mathbb{E}^*$ maps the volume average of the strains $\boldsymbol{\varepsilon}$ on the volume average of the stress $\boldsymbol{\sigma}$.

$$\langle \boldsymbol{\sigma} \rangle_\Omega = \mathbb{E}^* : \langle \boldsymbol{\varepsilon} \rangle_\Omega \tag{1}$$

where $\langle \cdot \rangle = \frac{1}{|\Omega|} \int_\Omega \cdot \, \mathrm{d}\Omega$. This also holds in the nonlinear range where $\mathbb{E}^*$ depends on the deformation and maybe the deformation path itself. Unfortunately a requirement for the strain measure in (1) is linearity in the displacements, also for the geometrically nonlinear theory as will be seen in the next section.

2.1 Average Strain Theorem for Finite Deformations

The average strain theorem shows that for a perfectly bonded RVE under a uniform displacement boundary condition the volume average of the deformation is the same as the given deformation on the boundary. In finite deformations the deformation can be described by the deformation gradient $\boldsymbol{F}$. Linear displacements prescribed on the boundary lead to a constant displacement gradient $\boldsymbol{\mathcal{H}}$.

$$\boldsymbol{u}|_{\partial\Omega_0} = \boldsymbol{\mathcal{H}} \cdot \boldsymbol{X} \qquad \boldsymbol{\mathcal{H}} = \mathrm{const} \tag{2}$$

The strains can be measured by the deformation gradient which is given on the boundary by

$$\boldsymbol{F}|_{\partial\Omega_0} = \left.\frac{\partial \boldsymbol{x}}{\partial \boldsymbol{X}}\right|_{\partial\Omega_0} = \mathbf{1} + \left.\frac{\partial \boldsymbol{u}}{\partial \boldsymbol{X}}\right|_{\partial\Omega_0} = \mathbf{1} + \boldsymbol{\mathcal{H}} = \boldsymbol{\mathcal{F}} \qquad . \tag{3}$$

The volume average of the deformation gradient yields

$$\langle \boldsymbol{F} \rangle_{\Omega_0} = \frac{1}{|\Omega_0|} \int_{\Omega_0} \boldsymbol{F} \, \mathrm{d}\Omega_0 = \mathbf{1} + \frac{1}{|\Omega_0|} \left(\int_{\Omega_0^1} \frac{\partial \boldsymbol{u}}{\partial \boldsymbol{X}} \, \mathrm{d}\Omega_0^1 + \int_{\Omega_0^2} \frac{\partial \boldsymbol{u}}{\partial \boldsymbol{X}} \, \mathrm{d}\Omega_0^2 \right) \tag{4}$$

where Ω_0^α are the volumes of the respective material phases in the undeformed configuration.

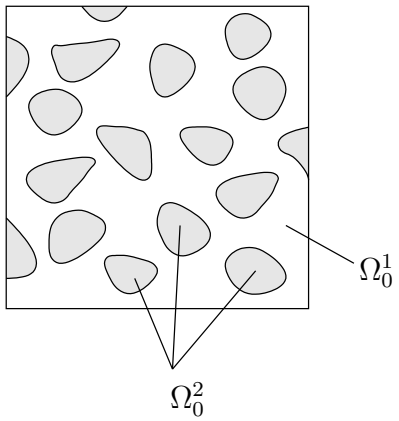

Figure 1: Scheme of a microstructure

It can be shown that for the boundary conditions given in (2) we obtain

$$\langle \boldsymbol{F} \rangle_{\Omega_0} = \boldsymbol{\mathcal{F}} + \frac{1}{|\Omega_0|} \int_{\partial\Omega_0^1 \cap \partial\Omega_0^2} [\![\boldsymbol{u}]\!] \otimes \boldsymbol{n}_0 \, \mathrm{d}\partial\Omega_0^{1,2} \qquad . \tag{5}$$

where $[\![\boldsymbol{u}]\!]$ is the jump within the displacement field in case of a not perfectly bonded microstructure. In case of a perfectly bonded microstructure the displacement jumps vanish. Then

$$\langle \boldsymbol{F} \rangle_{\Omega_0} = \boldsymbol{\mathcal{F}} \qquad . \tag{6}$$

In a very similar way one can derive that in case of $[\![\dot{\boldsymbol{u}}]\!] \equiv 0$ it holds

$$\langle \dot{\boldsymbol{F}} \rangle_{\Omega_0} = \dot{\boldsymbol{\mathcal{F}}} \qquad . \tag{7}$$

2.2 Average Stress Theorem

The average stress theorem states that in the absence of body forces and under a uniform load at the boundary the volume average stress is the same as the given stress at the boundary. For finite deformations we have to distinguish between different configurations. The average stress theorem can be derived for both, the initial as well as the current configuration. In this paper we restrict ourselves to the derivation with respect to the initial configuration. We assume a constant stress vector on the surface, given by Cauchy's theorem

$$\boldsymbol{t}|_{\partial\Omega_0} = \boldsymbol{\mathcal{P}} \cdot \boldsymbol{n}_0 \qquad \boldsymbol{\mathcal{P}} = \text{const}, \tag{8}$$

where $\boldsymbol{\mathcal{P}}$ is the first Piola Kirchhoff stress tensor and $\boldsymbol{n}_0$ is the unit normal vector on the surfaces of the RVE in the initial configuration. The equations of motion in this configuration are

$$\text{Div}\boldsymbol{P} + \boldsymbol{f}_0 = \boldsymbol{0} \tag{9}$$

where Div is the divergence operator with respect to the Lagrangian coordinates, $\boldsymbol{P}$ is the field of first Piola Kirchhoff stresses within the RVE and $\boldsymbol{f}_0$ is the body force in the initial configuration. Using (9) it can be shown that

$$\text{Div}(\boldsymbol{X} \otimes \boldsymbol{P}) = \boldsymbol{P}^T - \boldsymbol{X} \otimes \boldsymbol{f}_0 \qquad . \tag{10}$$

This result is now used to derive an expression for the volume average of the transposed of the first Piola Kirchhoff stress tensor

$$\langle \boldsymbol{P}^T \rangle_{\Omega_0} = \frac{1}{|\Omega_0|} \int\limits_{\Omega_0} \boldsymbol{P}^T \, \mathrm{d}\Omega_0 = \frac{1}{|\Omega_0|} \int\limits_{\Omega_0} (\text{Div}(\boldsymbol{X} \otimes \boldsymbol{P}) + \boldsymbol{X} \otimes \boldsymbol{f}_0) \, \mathrm{d}\Omega_0 \qquad . \tag{11}$$

Using the divergence theorem and the fact that on the surface $\boldsymbol{P} = \boldsymbol{\mathcal{P}}$ we obtain

$$\langle \boldsymbol{P}^T \rangle_{\Omega_0} = \frac{1}{|\Omega_0|} \left(\int\limits_{\partial\Omega_0} \boldsymbol{X} \otimes \boldsymbol{\mathcal{P}} \cdot \boldsymbol{n}_0 \, \mathrm{d}\partial\Omega_0 + \int\limits_{\Omega_0} \boldsymbol{X} \otimes \boldsymbol{f}_0 \, \mathrm{d}\Omega_0 \right) \qquad . \tag{12}$$

By applying the divergence theorem again the first term yields the constant stress, hence

$$\langle \boldsymbol{P}^T \rangle_{\Omega_0} = \boldsymbol{\mathcal{P}}^T + \frac{1}{|\Omega_0|} \int\limits_{\Omega_0} \boldsymbol{X} \otimes \boldsymbol{f}_0 \, \mathrm{d}\Omega_0 \tag{13}$$

which for zero body forces yields

$$\langle \boldsymbol{P} \rangle_{\Omega_0} = \boldsymbol{\mathcal{P}} \qquad . \tag{14}$$

2.3 Hill's Theorem for Finite Deformations

A commonly accepted criterion for the choice of the size of the RVE is Hill's condition which states that

$$\langle \boldsymbol{\sigma} : \boldsymbol{\varepsilon} \rangle_\Omega = \langle \boldsymbol{\sigma} \rangle_\Omega : \langle \boldsymbol{\varepsilon} \rangle_\Omega \tag{15}$$

in case the body is perfectly bonded and there are no body forces. This leads to the fact that the RVE has to be small enough such that from the macroscopic point of view the strain and the stress of the macroscopic body can be assumed to be approximately constant at the location of the RVE. Due to that the RVE can be regarded as one point of the macroscopic structure. On the other hand the RVE has to be large enough such that the boundary field fluctuations are relatively small. In linear theory it is simple to show that the volume average of the infinitesimal strain tensor $\langle \boldsymbol{\varepsilon} \rangle_\Omega$ is equal to the infinitesimal strain tensor at the boundary of the RVE. For nonlinear strain measures like Green's strain tensor $\boldsymbol{E} = \frac{1}{2}(\boldsymbol{F}^T\boldsymbol{F} - \boldsymbol{1})$ this is not possible. This equality can only be fulfilled by deformation measures which are linearly dependent on the displacement like the deformation gradient $\boldsymbol{F}$. It is convenient to derive Hill's theorem for finite deformations by using the stress power instead of the strain energy. Then, it can be formulated in the current configuration as well as in the initial configuration. Since both derivations

are very similar we restrict ourselves to the initial configuration. Using (10) we obtain

$$\begin{aligned}\int_{\Omega_0} \boldsymbol{P} : \dot{\boldsymbol{F}}\,\mathrm{d}\Omega_0 &= \int_{\Omega_0} \mathrm{Div}\,(\dot{\boldsymbol{x}}\cdot\boldsymbol{P})\,\mathrm{d}\Omega_0 + \int_{\Omega_0} \dot{\boldsymbol{x}}\cdot\boldsymbol{f}_0\,\mathrm{d}\Omega_0 \\ &= \int_{\partial\Omega_0^1} \dot{\boldsymbol{x}}\cdot\boldsymbol{t}_0\,\mathrm{d}\partial\Omega_0^1 + \int_{\partial\Omega_0^2} \dot{\boldsymbol{x}}\cdot\boldsymbol{t}_0\,\mathrm{d}\partial\Omega_0^2 \\ &+ \int_{\partial\Omega_0^1\cap\partial\Omega_0^2} [\![\dot{\boldsymbol{x}}]\!]\cdot\boldsymbol{t}_0\,\mathrm{d}\partial\Omega_0^{1,2} + \int_{\Omega_0} \dot{\boldsymbol{x}}\cdot\boldsymbol{f}_0\,\mathrm{d}\Omega_0\end{aligned} \tag{16}$$

This equation can be evaluated for the Neumann boundary conditions $\boldsymbol{t}|_{\partial\Omega_0} = \boldsymbol{\mathcal{P}}\cdot\boldsymbol{n}_0$ leading to the average stress power

$$\begin{aligned}\langle \boldsymbol{P} : \dot{\boldsymbol{F}}\rangle_{\Omega_0} &= \frac{1}{|\Omega_0|}\int_{\Omega_0} \boldsymbol{P} : \dot{\boldsymbol{F}}\,\mathrm{d}\Omega_0 \\ &= \ldots \\ &= \boldsymbol{\mathcal{P}} : \langle\dot{\boldsymbol{F}}\rangle_{\Omega_0} + \frac{1}{|\Omega_0|}\left(\int_{\partial\Omega_0^1\cap\partial\Omega_0^2} [\![\dot{\boldsymbol{x}}]\!]\cdot\boldsymbol{\mathcal{P}}\cdot\boldsymbol{n}_0\,\mathrm{d}\partial\Omega_0^{1,2} + \int_{\Omega_0}\dot{\boldsymbol{x}}\cdot\boldsymbol{f}_0\,\mathrm{d}\Omega_0\right)\end{aligned} \tag{17}$$

Again, if $\boldsymbol{f}_0 \equiv \boldsymbol{0}$ and $[\![\dot{\boldsymbol{x}}]\!] \equiv \boldsymbol{0}$ it follows with (14) $\langle \boldsymbol{P} : \dot{\boldsymbol{F}}\rangle_{\Omega_0} = \langle\boldsymbol{P}\rangle_{\Omega_0} : \langle\dot{\boldsymbol{F}}\rangle_{\Omega_0}$

For Dirichlet boundary conditions $\dot{\boldsymbol{x}}|_{\partial\Omega_0} = \dot{\boldsymbol{\mathcal{F}}}\cdot\boldsymbol{X}$ we have

$$\begin{aligned}\langle \boldsymbol{P} : \dot{\boldsymbol{F}}\rangle_{\Omega_0} &= \frac{1}{|\Omega_0|}\int_{\Omega_0} \boldsymbol{P} : \dot{\boldsymbol{F}}\,\mathrm{d}\Omega_0 \\ &= \ldots \\ &= \langle\boldsymbol{P}\rangle_{\Omega_0} : \dot{\boldsymbol{\mathcal{F}}} + \frac{1}{|\Omega_0|}\int_{\partial\Omega_0^1\cap\partial\Omega_0^2} [\![\dot{\boldsymbol{x}}]\!]\cdot\boldsymbol{P}\cdot\boldsymbol{n}_0\,\mathrm{d}\partial\Omega_0^{1,2}\end{aligned} \tag{18}$$

which means in case of $[\![\dot{\boldsymbol{x}}]\!] \equiv \boldsymbol{0}$ we have, based on (7), $\langle \boldsymbol{P} : \dot{\boldsymbol{F}}\rangle_{\Omega_0} = \langle\boldsymbol{P}\rangle_{\Omega_0} : \langle\dot{\boldsymbol{F}}\rangle_{\Omega_0}$

3 Material Model

The microstructure consists of randomly distributed spherical particles embedded in a binding matrix. The delamination process is restricted to a domain around the particles, see figure 2. This zone is also called “cohesive zone”. Further details about the cohesive zone approach can be found for example in Needleman (1993).

The material chosen for the matrix material and the particle material is a simple kompressible Neo-Hooke material with the strain energy function

$$\psi^{(\beta)} = \frac{\mu^{(\beta)}}{2}\left(I_{\boldsymbol{b}} - 3\right) - \mu^{(\beta)}\ln(J) + \frac{\lambda^{(\beta)}}{4}\left(J^2 - 1 - 2\ln(J)\right) \qquad \beta = 1,2 \qquad , \tag{19}$$

where $\beta = 1$ indicates the matrix material and $\beta = 2$ the particle material. The first Piola-Kirchhoff stress tensor for the two materials follow from

$$\boldsymbol{P}^{(\beta)} = \frac{\partial\psi^{(\beta)}}{\partial\boldsymbol{F}} \tag{20}$$

which yields

$$\boldsymbol{P}^{(\beta)} = \mu^{(\beta)}\left(\boldsymbol{F} - \boldsymbol{F}^{-T}\right) + \frac{\lambda^{(\beta)}}{2}\left(J^2 - 1\right)\boldsymbol{F}^{-T} \qquad , \tag{21}$$

where $I_{\boldsymbol{b}}$ is the first invariant of the left Cauchy-Green tensor, $J = \det\boldsymbol{F}$, and $\mu^{(\beta)}$ and $\lambda^{(\beta)}$ are the Lamé parameters.

3.1 Damage Model for the Cohesive Zone

The material model for the cohesive zone is a simple damage model following the suggestion of Zohdi and Wriggers (2001). The undamaged material is also a kompressible Neo-Hooke material. Its material parameters are chosen to be a linear combination of the parameters of the matrix material and those of the particle material

$$\begin{aligned} \mu_0^{(\mathrm{cz})} &= \theta\mu^{(2)} + (1-\theta)\mu^{(1)} \\ \lambda_0^{(\mathrm{cz})} &= \theta\lambda^{(2)} + (1-\theta)\lambda^{(1)} \end{aligned} \tag{22}$$

θ is a parameter governing the stiffness of the undamaged cohesive zone material. The local degradation is represented by a variable α with $0 < \alpha \leq 1$ which "weakens" the stiffness of the material, which means that the material constants follow as

$$\begin{aligned} \mu^{(\mathrm{cz})} &= \alpha\mu_0^{(\mathrm{cz})} \\ \lambda^{(\mathrm{cz})} &= \alpha\lambda_0^{(\mathrm{cz})} \qquad . \end{aligned} \tag{23}$$

The local constraint condition from which α can be computed is

$$\Psi(\alpha) = \mathcal{M}(\alpha) - \mathcal{K}(\alpha) \leq 0 \tag{24}$$

where $\mathcal{M}(\alpha)$ is a scalar valued term representing the stress state of the material point

$$\mathcal{M}(\alpha) = \sqrt{\boldsymbol{g}(\boldsymbol{\sigma}_{\mathrm{deg}}(\alpha)) : \boldsymbol{g}(\boldsymbol{\sigma}_{\mathrm{deg}}(\alpha))} \tag{25}$$

$$\boldsymbol{g}(\boldsymbol{\sigma}_{\mathrm{deg}}(\alpha)) = \eta_1 \frac{\mathrm{tr}(\boldsymbol{\sigma}_{\mathrm{deg}})}{3}\mathbf{1} + \eta_2 \left(\boldsymbol{\sigma}_{\mathrm{deg}} - \frac{\mathrm{tr}(\boldsymbol{\sigma}_{\mathrm{deg}})}{3}\mathbf{1} \right) \tag{26}$$

and η_1 and η_2 are parameters scaling the isochoric and deviatoric parts of $\boldsymbol{g}(\boldsymbol{\sigma}_{\mathrm{deg}}(\alpha))$. $\mathcal{K}(\alpha)$ is a threshold value which depends on the damage variable α itself.

$$\mathcal{K}(\alpha) = \Phi_{\mathrm{lim}} + (\Phi_{\mathrm{crit}} - \Phi_{\mathrm{lim}})\,\alpha^P \tag{27}$$

Φ_{crit} is the initial threshold value, and Φ_{lim} is the threshold value in the limiting case that the material point has degraded completely ($\alpha = 0$). Finally P is an exponent which controls the rate of degradation.

4 Numerical Model

4.1 Discretisation

The RVE is chosen to be a cube. The distribution of the inclusions has to be random in order to be statistically representative. In three dimensions it is not easy to generate a mesh of only hexahedra elements approximating the boundaries of the inclusions accurately. In general those meshes would contain quite a lot of heavily distorted elements which would be extremely bad for the numerical solving process and the accuracy of the solution. A tetrahedra mesh would avoid this disadvantage, but linear tetrahedra elements are locking and lead to a much worse finite element solution. Quadratic tetrahedra are also quite bad in case of large deformations. These problems motivate a discretisation only with linear cube shaped hexahedra which of course is ideal for the equation solver but also approximates the geometry much less accurately. To increase the discretisation accuracy we refine the mesh with non-conforming elements close to the interfaces between the particles and the cohesive zones and the cohesive zones and the matrix material. This refinement also has the advantage that the error due to large stress gradients especially close to the interfaces can be decreased. A scheme of this adaptive discretisation can be seen in figure 2.

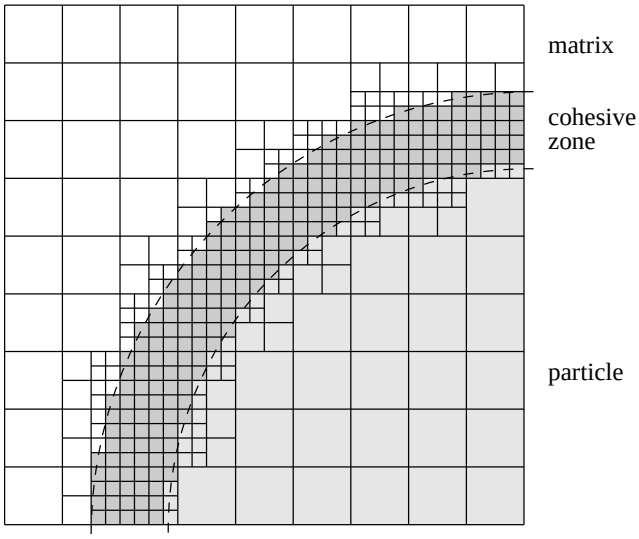

Figure 2: Discretisation with non-conforming cubic elements

4.2 Statistical Testing

Of course, to get a representative material response one has to do statistical tests with different random distributions of particles. Of special interest is the number of particles needed for each test, the refinement of the mesh and the number of tests which have to be computed to get a statistically representative result. The parameters for all tests are chosen to be

$$\begin{array}{rclrcl} \mu^{(1)} & = & 0.2 & \lambda^{(1)} & = & 0.3 \\ \mu^{(2)} & = & 2.0 & \lambda^{(2)} & = & 3.0 \\ \theta & = & 0.0 & & & \\ \eta_1 & = & 1.0 & \eta_2 & = & 1.0 \\ \Phi_{\mathrm{lim}} & = & 0.5 & \Phi_{\mathrm{crit}} & = & 1.0 \\ P & = & 0.1 & & & \end{array}$$

The particles all have a spherical shape and the same radius. The volume fraction of the inclusions is chosen to be 15%, and the thickness of the cohesive zone is $0.25\,r$, where r is the radius of each particle. Using these material parameters with the cohesive zone initially having the same properties as the matrix material one can observe that the thickness of the cohesive zone has almost no influence on the global response of the RVE. The displacements on the entire boundary of the RVE is given through the constant displacement gradient (see (2)) scaled by a load factor γ.

$$\boldsymbol{u}|_{\partial\Omega_0} = \gamma\,\boldsymbol{\mathcal{H}} \cdot \boldsymbol{X} \tag{28}$$

where $\boldsymbol{\mathcal{H}}$ is chosen to be

$$\boldsymbol{\mathcal{H}} = \begin{pmatrix} 1 & 1 & 1 \\ 1 & 1 & 1 \\ 1 & 1 & 1 \end{pmatrix} \tag{29}$$

4.2.1 Resolution of the Finite Element Mesh

To figure out the required resolution of the mesh we perform the test with only one inclusion and different mesh refinements. An example of a mesh is displayed in figure 3.

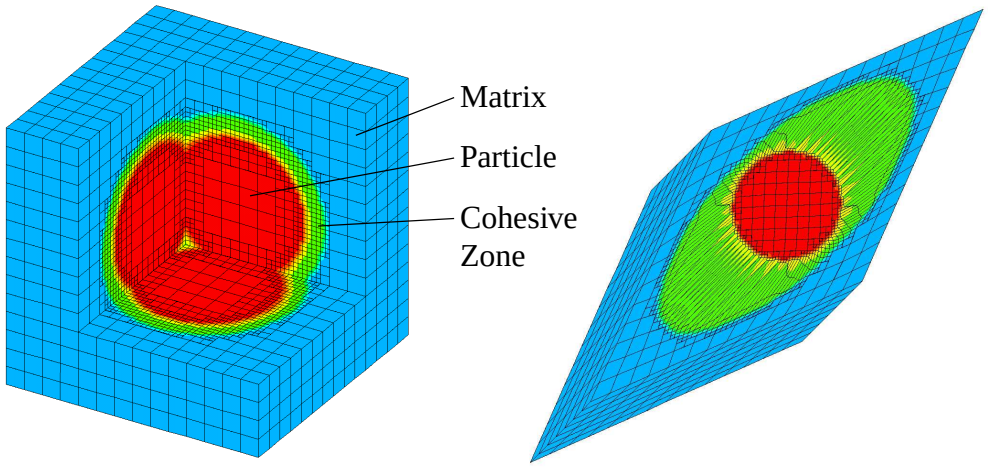

Figure 3: Finite element mesh: LEFT: undeformed RIGHT: deformed

The dependency of of the stored strain energy with respect to the number of degrees of freedom can be seen in figure 4.

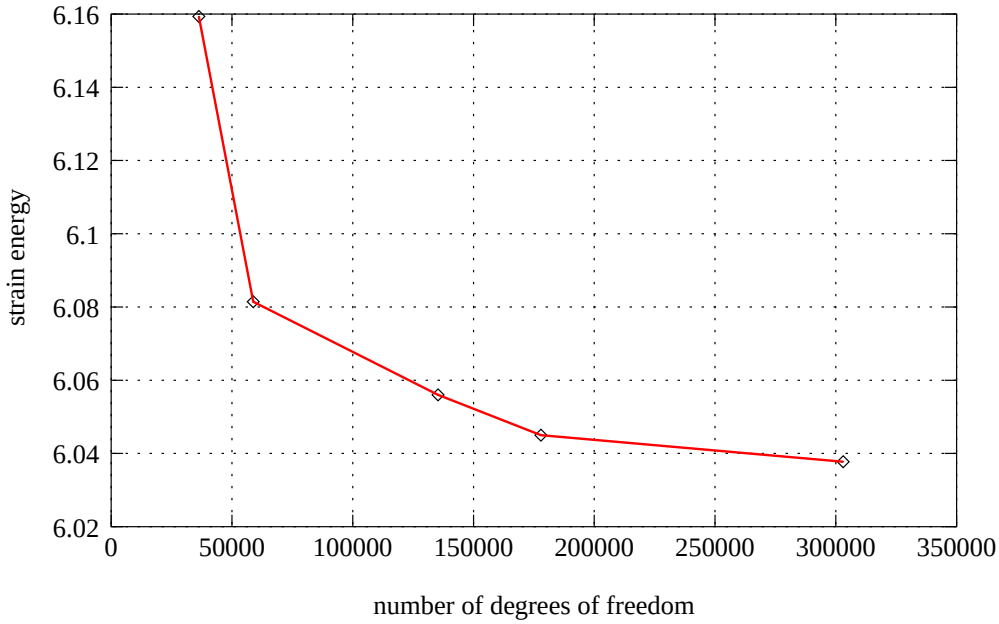

Figure 4: Convergence: overall energy

To decrease the computational effort to an acceptable amount, in the following we use a base resolution of $14 \times 14 \times 14$ elements and two subsequent subdivisions of the elements close to the cohesive zone. Compared to the finest resolution tested (1.78 million degrees of freedom) those results have an error of less than 1%.

4.2.2 Number of Inclusions

The necessary number of particles per test can be determined by an isotropy condition. Since the boundary conditions are the same in each of the base directions, an isotropic material must lead to an effective Cauchy stress response where

$$\sigma_{11} = \sigma_{22} = \sigma_{33} \tag{30}$$

and

$$\sigma_{12} = \sigma_{23} = \sigma_{31} \quad . \tag{31}$$

This can be used to test whether the number of inclusions is high enough for this specific test to give a representative result. A scalar measure for the deviation from isotropy of the effective material under isotropic loading conditions

is

$$e_{iso} = \big((\sigma_{11}-\sigma_{22})^2+(\sigma_{22}-\sigma_{33})^2+(\sigma_{33}-\sigma_{11})^2 + (\sigma_{12}-\sigma_{23})^2+(\sigma_{23}-\sigma_{31})^2+(\sigma_{31}-\sigma_{12})^2\big)^{\frac{1}{2}} \quad (32)$$

A plot of the mean value of e_{iso} as a function of the number of inclusions for a statistically representative number of tests for each number of inclusions is displayed in figure 5.

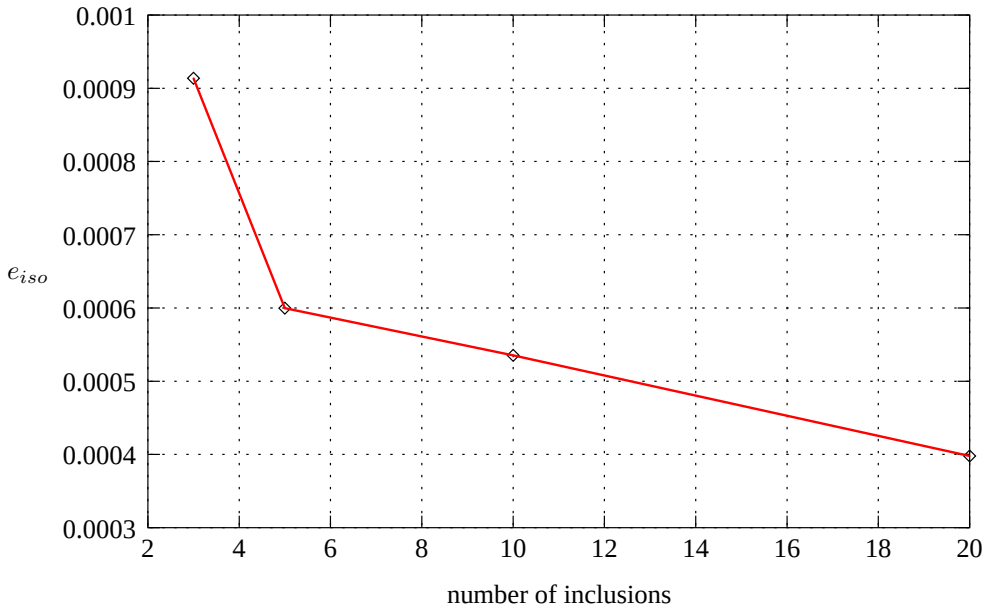

Figure 5: Deviation from isotropy

Another test to figure out the required number of inclusions is to look at the standard deviation of the stress response for multiple tests with the same number of inclusions. This value does not decrease with the number of tests performed. Only the number of inclusions per test has an impact on it. Still, to get a statistical representative material behaviour it is necessary to compute the same test many times with a different random distribution of the inclusions. Each of these tests yield an effective stress and strain response. The statistical representative effective response can be obtained by averaging all the effective stresses and strains for each load step over all the tests performed. From figure 6 which shows the standard deviation of the effective stresses it can be seen that a relatively low number of inclusions is sufficient to obtain a statistically representative result.

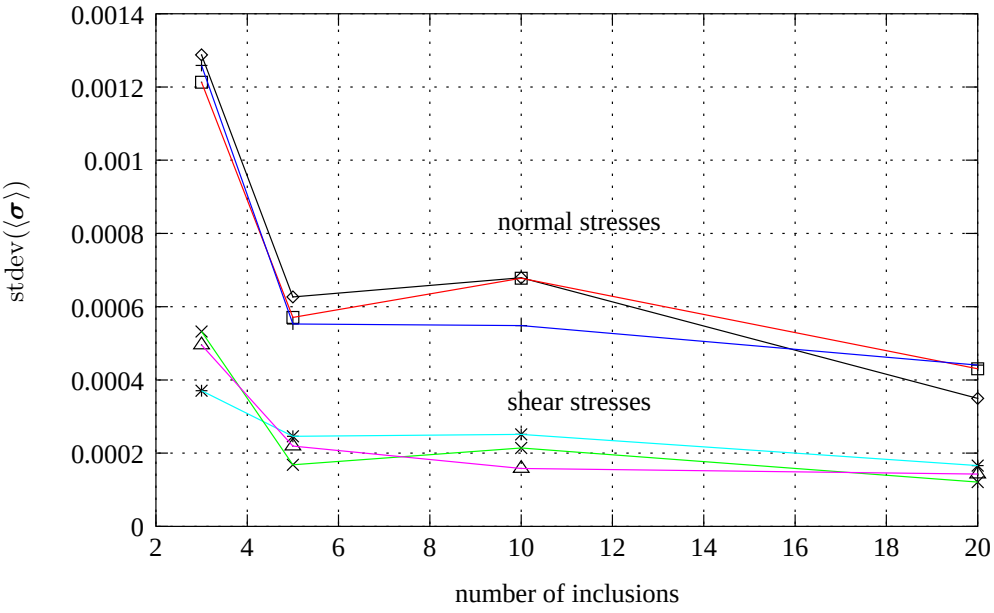

Figure 6: Standard deviation of the effective stresses

4.2.3 Number of Tests

At last the number of tests which have to be computed to get a statistically representative result is investigated. It is not possible to increase the accuracy of the effective response by computing more tests. But at a higher number of tests performed the collection of the effective results of each test form a more Gaussian distribution of the effective results. This is shown in the histograms in figure 7 and figure 8.

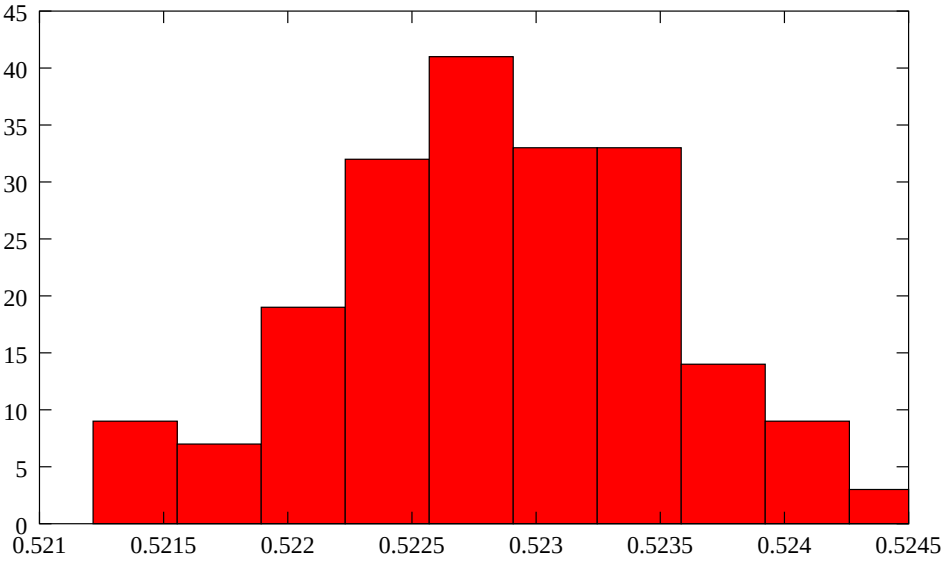

Figure 7: Histogram for effective Cauchy stress component $\langle \sigma_{11} \rangle$

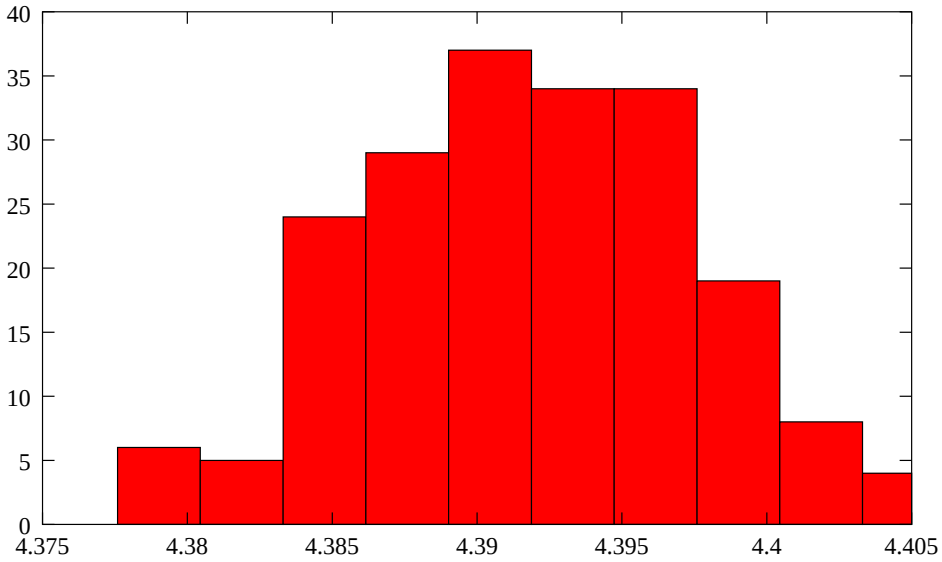

Figure 8: Histogram for stored energy

The actual averaged effective Cauchy stresses as a function of the load factor γ which is representative for the effective strains is shown in figure 9 for a loading and unloading test, and a typical deformed RVE with the damage parameter is displayed in figure 10.

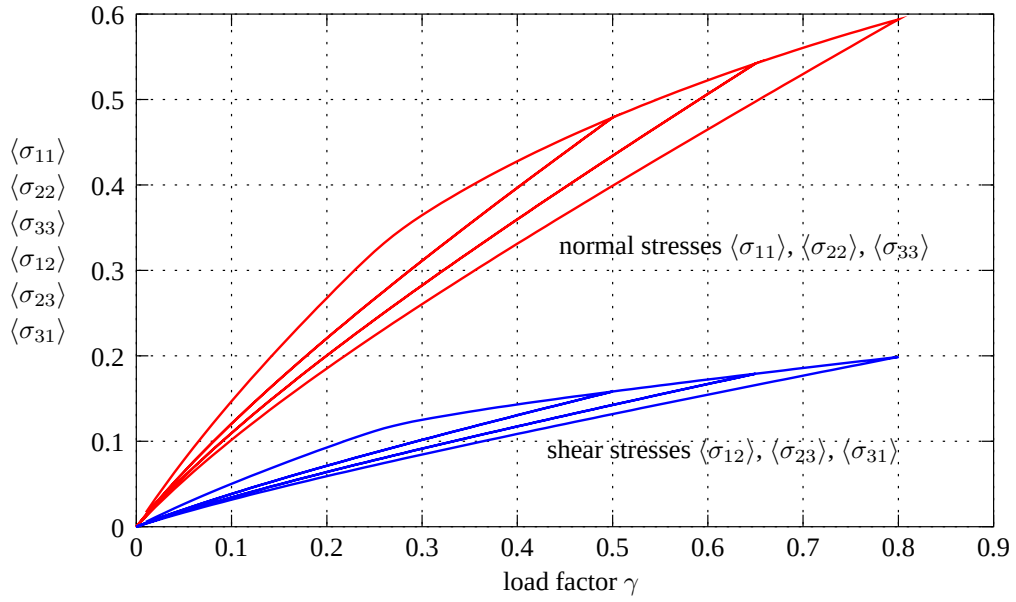

Figure 9: Average effective stresses as a function of the load parameter γ

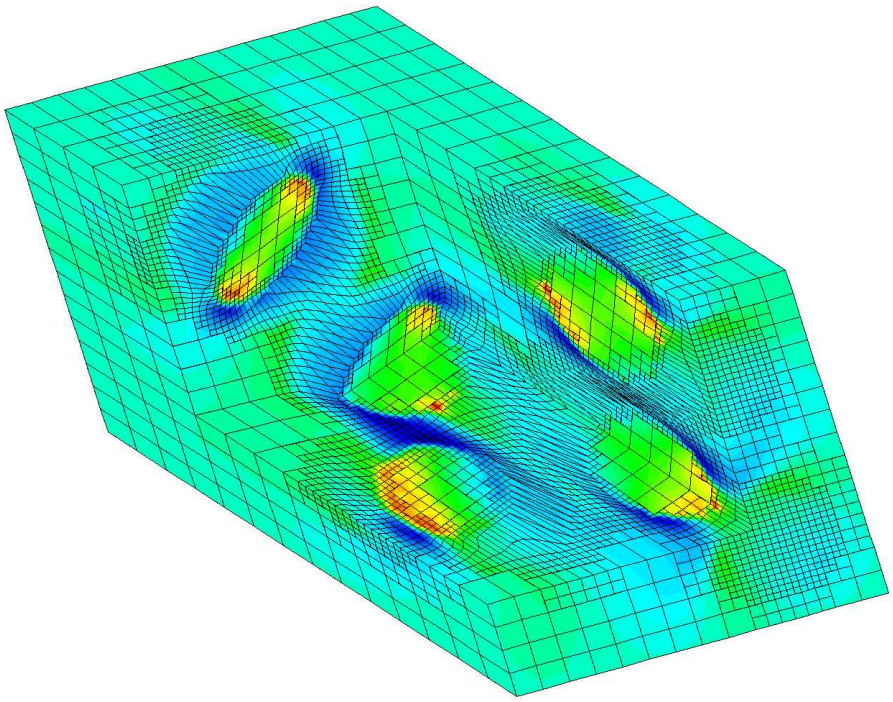

Figure 10: First principal stress of a typical RVE with damage in the cohesive zone

5 Conclusions

In this paper we presented some background information about averaging and homogenisation techniques at finite deformations. We applied those techniques to a RVE consisting of a soft matrix material and stiffer spherical shaped inclusions. In a cohesive zone connecting the matrix material and the particles we applied a simple damage law to model delamination at finite strains. Computational and statistical aspects are shown. Future work will be directed at the implementation of a more complex delamination law which is able to model certain local effects more detailed. A big issue is the provision of a material law for the effective material response of the RVE which is difficult and subject to research even for the nonlinear but purely elastic range.

References

Bishop, J.; Hill, R.: A theoretical derivation of the plastic properties of a polycrystalline face-centred matal. *Phil. Mag.*, 42, (1951a), 1298–1307.

Bishop, J.; Hill, R.: A theory of the plastic distortion of a polycrystalline aggregate under combined stresses. *Phil. Mag.*, 42, (1951b), 414–427.

Eshelby, J.: The elastic field of an ellipsoidal includion, and related problems. *Proc. Roy. Soc.*, A241, (1957), 376–396.

Hashin, Z.; Shtrikman, S.: On some variational principles in anisotropic and nonhomogeneous elasticity. *Journal of the Mechanics and Physics of Solids.*, 10, (1962), 335–342.

Hill, R.: The elastic behaviour of a crystalline aggregate. In: *Proc. Phys. Soc. (Lond.)*, A65, pages 349–354 (1952).

Mori, T.; Tanaka, K.: Average stress in matrix and average energy of materials with misfitting inclusions. *Acta Metall.*, 21, (1973), 571–574.

Needleman, A. e. a.: Matrix reinforcement, and interfacial failure. In: M. A. Suresh, S.; A. Needleman, eds., *Fundamentals of metal matrix composites*, Butterworth-Heineman publishers (1993).

Reuss, A.: Berechnung der Fliessgrenze von Mischkristallen auf Grund der Plastizitätsbedingung für Einkristalle. *Z. angew. Math. Mech.*, 9, (1929), 49–58.

Voigt, W.: Über die Beziehung zwischen den beiden Elastizitätskonstanten isotroper Körper. *Wied. Ann.*, 38, (1889), 573–587.

Zohdi, T.; Wriggers, P.: Computational micro-macro material testing. *Archives of Computational Methods in Engineering.*, 8, 2, (2001), 131–228.

Address: S. Löhnert, P. Wriggers
Institute of Mechanics and Computational Mechanics
University of Hannover
Appelstr. 9a, 30167 Hannover
email: `loehnert@ibnm.uni-hannover.de`